

See discussions, stats, and author profiles for this publication at: <https://www.researchgate.net/publication/243867631>

Ab initio Study of Electronic Structure and Properties in Crystalline 1,1,3,3,5,5-Hexaazidocyclotriphosphazene

ARTICLE *in* CHINESE JOURNAL OF CHEMISTRY · MAY 2008

Impact Factor: 1.58 · DOI: 10.1002/cjoc.200890158

CITATION

1

READS

14

5 AUTHORS, INCLUDING:



Jian-Guo Zhang

Beijing Institute of Technology

312 PUBLICATIONS 1,577 CITATIONS

SEE PROFILE



Tong-Lai Zhang

Beijing Institute of Technology

271 PUBLICATIONS 1,131 CITATIONS

SEE PROFILE



Li Yang

China Medical University (PRC)

138 PUBLICATIONS 2,380 CITATIONS

SEE PROFILE

Ab initio Study of Electronic Structure and Properties in Crystalline 1,1,3,3,5,5-Hexaazidocyclotriphosphazene

HUANG, Hui-Sheng(黄辉胜) ZHANG, Jian-Guo(张建国) ZHANG, Tong-Lai*(张同来)
YANG, Li(杨利) ZHENG, Hui-Hui(郑慧慧)

State Key Laboratory of Explosion Science and Technology, Beijing Institute of Technology, Beijing 100081, China

The banding and electronic structures of crystalline 1,1,3,3,5,5-hexaazidocyclotriphosphazene (P_3N_{21}) have been investigated at DFT-B3LYP/6-31G(d) level. Relaxed crystal structure compares well with experimental data. The energy gap is 5.57 eV, indicating that P_3N_{21} is an insulator. The frontier orbital is mainly formed by atomic orbitals of azido group, so it is the most reactive part of the molecule. The intermolecular interaction is strong along the direction that is nearly perpendicular to the phosphazene ring. The distribution of electrostatic potential is quite uneven, so P_3N_{21} has a very high impact sensitivity. The point charge electrostatic potential is very high between the azido groups of the neighboring molecules, which indicates that the crystal lattice in this position may easily be broken and becomes the explosion center when P_3N_{21} is impacted. The overlap populations of P—N _{α} bonds are much less than those of other bonds, therefore the P—N _{α} bonds first rupture by external stimuli, which agrees well with the experimental study of mass spectrum.

Keywords phosphazene compound, density functional theory, band structure, electronic structure, electrostatic potential

Introduction

Phosphazene compounds attract many researchers for a long time due to their unique properties.^{1–9} For example, the energetic phosphazene compounds without heavy metal elements are environmentally friendly and have very high energy density. In 1954, Grundmann *et al.*³ first reported the synthesis of P_3N_{21} compound through the reaction of hexachlorophosphazene with sodium azide, but the title compound has only been characterized by elemental analysis. In 1970, R  uchle *et al.*⁵ prepared P_3N_{21} and the IR spectrum was obtained. In the assignment of the IR bands, it was assumed that the molecule had a D_{3h} point symmetry. After several years, M  ller *et al.*⁷ reported the synthesis of P_3N_{21} compound again, and characterized it by vibrational and NMR spectroscopy.

The P_3N_{21} compound is extremely sensitive, therefore, the first structural characterization through the single-crystal X-ray diffraction was made until 2006 by G  bel *et al.*⁹ In addition, they investigated the IR, Raman, NMR and MS spectroscopy, also DSC and sensitivity properties. The vibrational frequencies were assigned by comparison with the frequencies calculated for a molecule of C_1 point symmetry. And P_3N_{21} has a very high impact sensitivity at room temperature (<1 J), and direct heating in a flame also results in an explosive decomposition of the compound with a loud noise and a flash of light. Furthermore, the isolated molecule of

P_3N_{21} was calculated at BLYP/6-31G(d) and B3LYP/6-31G(d) level, and both the IR and Raman spectra were calculated which compare well with the experimental frequencies.

As far as we know, the present paper represents the first *ab initio* fully periodic SCF study of crystalline P_3N_{21} . Herein, the periodic DFT calculation at B3LYP/6-31G(d) level was performed on a P_3N_{21} crystal. The banding and electronic structures were investigated and the relationship between structure and property was discussed.

Computational details

Both the P_3N_{21} molecule and its bulk were fully optimized and the C_1 point symmetry was adopted when optimizing the molecule. The hybrid density functional method including Becke's 3-parameter nonlocal exchange functional¹⁰ with the correlation functional of Lee-Yang-Parr¹¹ (B3LYP) was employed for the calculations. The method makes the electron correlation included and is still computationally economic. At the same time, the split valence 6-31G(d) basis set was used for N and P atoms. Computational practice for a molecular crystal showed that the energy was essentially constant from the 6-21G level.¹²

The crystal structure obtained from the X-ray diffraction was used for the computation of the bulk. The molecular structure and crystal structure of P_3N_{21} are

* E-mail: ztlbit@bit.edu.cn; Tel. and Fax: 0086-010-68913818

Received November 21, 2007; revised December 13, 2007; accepted January 17, 2008.

Project supported by the National Natural Science Foundation of China (No. 10776002).

shown in Figure 1, and the unit cell was found to be $a = 0.7195$ nm, $b = 0.7372$ nm, $c = 1.2994$ nm, $\alpha = 87.41^\circ$, $\beta = 78.95^\circ$ and $\gamma = 89.59^\circ$, crystallizing in the space group $P\bar{1}$ with two formula units per unit cell. The three azido groups of N(4)—N(5)—N(6), N(10)—N(11)—N(12), and N(19)—N(20)—N(21) are nearly parallel to the phosphazene ring, and the three remaining azido groups of N(7)—N(8)—N(9), N(13)—N(14)—N(15), and N(16)—N(17)—N(18) are nearly perpendicular to the ring. The six-membered ring is not absolutely planar and takes a slight chair conformation.⁹ For the periodic calculation, both high quality basis set and large enough k points should be adopted. Due to the periodicity of the lattice, the calculated orbital energies will depend on the crystal orbital wave vector k . Therefore 260 k points were adopted in reciprocal space for the periodic calculation. The Monkhorst shrinking factor¹³ for the periodic calculations is 8. The threshold for energy convergence is 10^{-8} a.u. in both periodic and nonperiodic calculations.

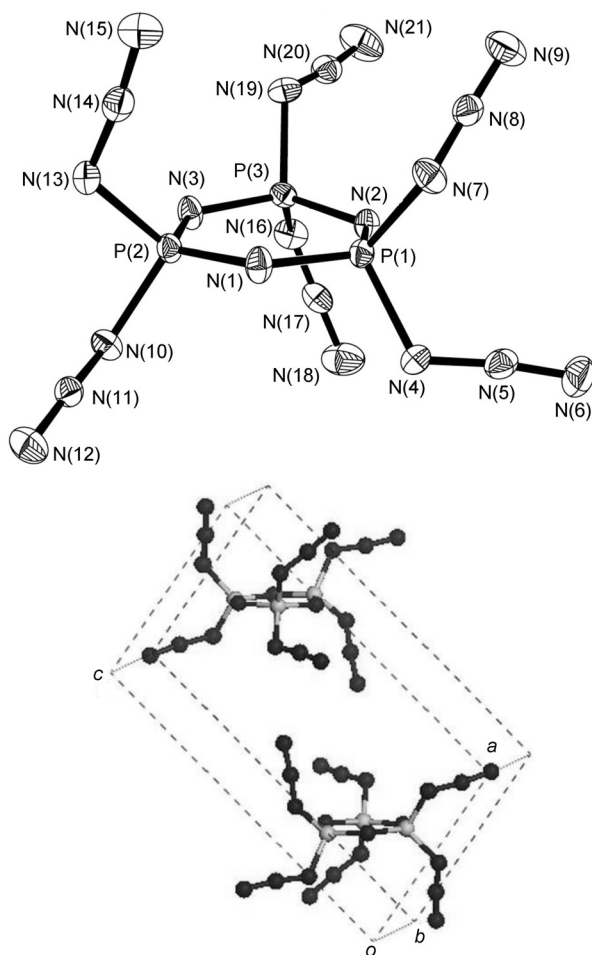


Figure 1 Molecular structure and crystal structure of P_3N_{21} .

The crystal lattice energy is defined as the total energy of the bulk minus that of gaseous molecule.¹⁴ To obtain the lattice energy more reasonably, we optimized the geometries for both the isolated molecule and the

bulk. Moreover, the atomic charge, overlap population, electrostatic potential, band structure and density of states were calculated with the optimized geometries. All the calculations employed the CRYSTAL06 suite of programs.¹⁵

Results and discussion

Bulk properties

The calculated lattice parameters, bond lengths and bond angles of P_3N_{21} are given in Table 1 together with its experimental values.⁹ It can be seen that both the calculated lattice constants and the internal structure parameters of P_3N_{21} assigned by the bond lengths and bond angles are close to the corresponding experimental data as shown in Table 1. These comparisons confirm that our computational parameters are reasonably satisfactory.

Charge distribution

The atomic charges of a P_3N_{21} molecule and its bulk at the B3LYP/6-31G(d) level are listed in Table 2. It can be seen that the atomic charge distribution in the molecule is similar to that in the bulk, but the atomic charges in the bulk are less evenly distributed than those in the molecule, indicating that there is intermolecular interaction between molecules in the bulk of P_3N_{21} . Table 2 shows that all the phosphorus atoms bear almost 1 a.u. positive charge, respectively. However, nitrogen atoms that connected with the phosphorus atom, both the N_{ring} and the N_α (attached to the ring) carry negative charge. This maybe results from that the electronegativity of nitrogen atom is stronger than that of the phosphorus atom. In addition, the N_β (central N of the azido group) atom carries 0.448–0.476 a.u. positive charge, while the N_γ (terminal N of the azido group) atom carries 0.206–0.243 a.u. negative charge in the bulk.

The projections of total charge density of the bulk (a) in the plane containing the three phosphorus atoms, and (b) perpendicular to the plane which contains the three phosphorus atoms are shown in Figure 2. It is not negligible that only five atoms are observed in the six-membered ring in Figure 2a, *i.e.*, there is a lack of one nitrogen atom, suggesting that the six-membered ring is not absolutely planar, which agrees well with the reference.⁹ It also can be seen from Figure 2a that there is no charge density in the intermolecular regions in the plane containing the three phosphorus atoms, indicating that the intermolecular interaction between the neighboring molecules along this direction in the bulk is very weak. In contrast, Figure 2b shows that a little charge density is overlapped for the azido groups of the neighboring molecules in the plane, thereby, the intermolecular interaction along this direction is stronger.

Overlap population analysis

The electronic structure can be further investigated by examining the overlap populations in the molecule

Table 1 Selected experimental (in parentheses) and relaxed lattice constants for P_3N_{21}

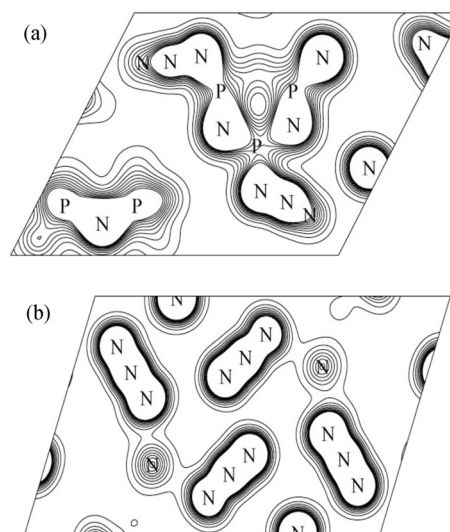
Lattice constant	Bond length/nm		Bond angle/(°)	
$a=0.7102$ (0.7195)	P(1)—N(1)	0.1547 (0.1558)	N(1)-P(1)-N(2)	118.73 (118.23)
$b=0.7469$ (0.7372)	P(1)—N(2)	0.1569 (0.1576)	N(1)-P(2)-N(3)	117.92 (117.09)
$c=1.2705$ (1.2994)	P(2)—N(1)	0.1527 (0.1570)	N(2)-P(3)-N(3)	116.04 (117.38)
$\alpha=85.79$ (87.41)	P(2)—N(3)	0.1595 (0.1567)	P(1)-N(1)-P(2)	120.36 (122.14)
$\beta=80.32$ (78.95)	P(3)—N(2)	0.1521 (0.1575)	P(1)-N(2)-P(3)	120.81 (120.88)
$\gamma=89.24$ (89.59)	P(3)—N(3)	0.1497 (0.1556)	P(2)-N(3)-P(3)	121.70 (122.93)
	P(1)—N(4)	0.1668 (0.1666)	N(1)-P(1)-N(4)	104.58 (104.50)
	P(1)—N(7)	0.1627 (0.1671)	N(2)-P(1)-N(4)	112.69 (111.87)
	N(4)—N(5)	0.1224 (0.1218)	N(1)-P(1)-N(7)	111.06 (108.91)
	N(5)—N(6)	0.1130 (0.1117)	N(2)-P(1)-N(7)	109.42 (109.83)
	N(7)—N(8)	0.1169 (0.1203)	P(1)-N(4)-N(5)	116.25 (117.70)
	N(8)—N(9)	0.1117 (0.1114)	P(1)-N(7)-N(8)	120.07 (119.17)
			N(4)-N(5)-N(6)	173.19 (173.40)
			N(7)-N(8)-N(9)	174.16 (173.50)

Table 2 Atomic charges (a.u.) of a P_3N_{21} molecule and its bulk

Atom	Charge	
	Molecule	Bulk
P	1.053—1.063	0.997—1.028
N _{ring}	−0.635—−0.589	−0.618—−0.587
N _{α}	−0.462—−0.445	−0.471—−0.416
N _{β}	0.434—0.439	0.448—0.476
N _{γ}	−0.208—−0.203	−0.243—−0.206

and bulk. The Mulliken overlap population is useful in evaluating the nature of bonds in a compound. Although the absolute magnitudes of Mulliken overlap populations have little physical meaning, the relative values can still offer some useful information. The bond lengths and overlap populations of a P_3N_{21} molecule and its bulk are listed in Table 3. We note that the distribution of bond length and overlap population in the molecule is similar to that of the bulk, that is, the bond length of N_β — N_γ bonds is the shortest, but that of the P — N_α bonds is the longest. In contrast, the overlap population of N_β — N_γ bonds is the biggest, but that of the P — N_α bonds is the smallest. However, most of the bond lengths are shorter and the overlap populations are stronger in the bulk than those in the isolated molecule, indicating that the molecule in the bulk is more stable than the isolated molecule.

Both in the isolated molecule and in the bulk, the overlap population of P — N_α bonds is the weakest. Although the Mulliken overlap populations fail to give reliable characterization of bond strength, it obviously reveals that the P — N_α bonds are the weakest, therefore, the P — N_α bonds first rupture by external stimuli. This is in agreement with the experimental study of mass spectrometry.⁹ In the mass spectrum, there are two signals: the first mass peak corresponds to the molecular peak, and the second to a species in which one azido

**Figure 2** The total charge density of the bulk P_3N_{21} : (a) in the plane containing the three phosphorus atoms, and (b) perpendicular to the plane containing the three phosphorus atoms. Contour intervals at $0.01 e \cdot \text{Bohr}^{-3}$.

group has been removed from the P_3N_{21} molecule, that is, the second mass peak corresponds to the decomposition product due to the breakdown of P — N_α bonds. It demonstrates that the strength of P — N_α bonds is the weakest in P_3N_{21} compound, so the detonation may be initiated by the breakdown of P — N_α bonds.

Lattice energy, band structure and density of states

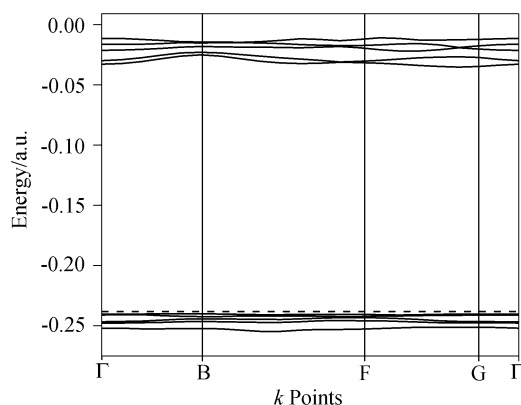
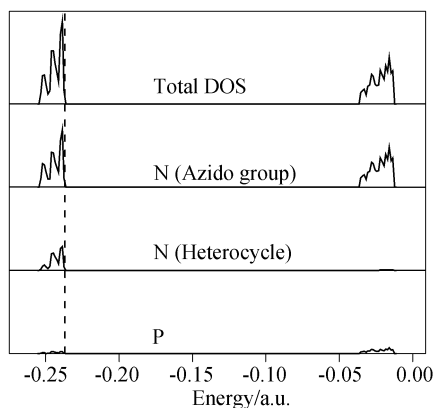
The total energy of the bulk is -5.70433129×10^6 kJ/mol, and that of gaseous molecules is -5.70430792×10^6 kJ/mol, so the calculated crystal lattice energy of P_3N_{21} is -23.37 kJ/mol at the B3LYP/6-31G(d) level.

The energy band structure of P_3N_{21} is shown in Figure 3, and the corresponding total and projected densities of states (DOS) are presented in Figure 4. As shown

Table 3 Bond lengths (nm) and Mulliken overlap populations of a P_3N_{21} molecule and its bulk

Bond	Bond length		Overlap population	
	Molecule	Bulk	Molecule	Bulk
P—N _{ring}	0.1598—0.1614	0.1497—0.1595	0.460—0.475	0.477—0.501
P—N _{α}	0.1699—0.1715	0.1627—0.1681	0.259—0.265	0.256—0.291
N _{α} —N _{β}	0.1242—0.1244	0.1140—0.1241	0.269—0.289	0.304—0.320
N _{β} —N _{γ}	0.1133—0.1134	0.1112—0.1136	0.590—0.596	0.623—0.679

in Figure 3, the frontier bands are slightly fluctuant, indicating that the molecular orbital is only slightly perturbed by the crystalline environment. It exhibits a large energy gap of 0.205 a.u. (5.57 eV) between valence and conduction bands, indicating that the crystal is an insulator. Both the highest occupied crystal orbital (HOCO) and the lowest unoccupied crystal orbital (LUCO) levels are degenerate. When small changes in the charge state occur, some orbitals are stabilized and others are destabilized, which eliminates the degeneracy of the HOCO and LUCO levels and could lead to minor Jahn-Teller distortions.^{16,17}

**Figure 3** Band structure of P_3N_{21} with 5 upper valence and 5 lower conduction bands. The Fermi energy is shown as a dashed line.**Figure 4** Projected and total density of states (DOS) of P_3N_{21} .

A better understanding of the character of these bands can be obtained by projecting the DOS on the atom-centered orbitals. As shown in Figure 4, the nitrogen atoms from azido groups mainly make up the va-

lence bands, also the nitrogen atoms from the heterocycle and phosphorus atoms have a little contribution, while the azido group N atoms make up the conduction bands, with very small contributions from phosphorus atoms. According to the above analysis, we can infer that the frontier orbital is mainly formed by atomic orbitals of the azido group, therefore, the azido group is the most reactive part of the molecule, which is in agreement with the fact.

Electrostatic potential

Let us consider electrostatic potential in the bulk of P_3N_{21} . The electrostatic potential is a property that is often used to analyze the electron density distribution in a molecule. Regions in which the electrostatic potential is positive indicate that it is “electron deficient”, *i.e.*, the electron density is low in that area. Regions in which the electrostatic potential is negative indicate that it is “electron rich”, *i.e.*, the electron density is higher in that region. It has been found by Politzer *et al.*^{18–20} and extensively used by Rice *et al.*²¹ that the computed electrostatic potential, in general, is related to the sensitivity of the bulk material.

The point charge electrostatic potentials of the bulk P_3N_{21} in the plane, a (100), b (010) and c (001) crystal-line faces are shown in Figure 5. We note that the distributions of electrostatic potentials on the three faces are all quite uneven. Obviously, there is a distinct interface between positive and negative electrostatic potentials. Additionally, the positive regions are larger and stronger than the negative ones. These would account for a very high impact sensitivity of P_3N_{21} at room temperature (<1 J).⁹ From the Figure 5c, we can see that the point charge electrostatic potential is positive and also very high between the azido groups of the neighboring molecules, which indicates that the crystal lattice in this position may easily be broken and becomes the explosion center when P_3N_{21} is impacted.²² Furthermore, this will result in breakdown of the P—N _{α} bonds and cause explosion.

Conclusion

In this study, a detailed *ab initio* study of the electronic structure of crystalline P_3N_{21} was performed at B3LYP/6-31G(d) level by a periodic DFT method. The results show that P_3N_{21} is an insulator, and the azido group is the most reactive part of the molecule. P_3N_{21} has a very high impact sensitivity, due to that the distri-

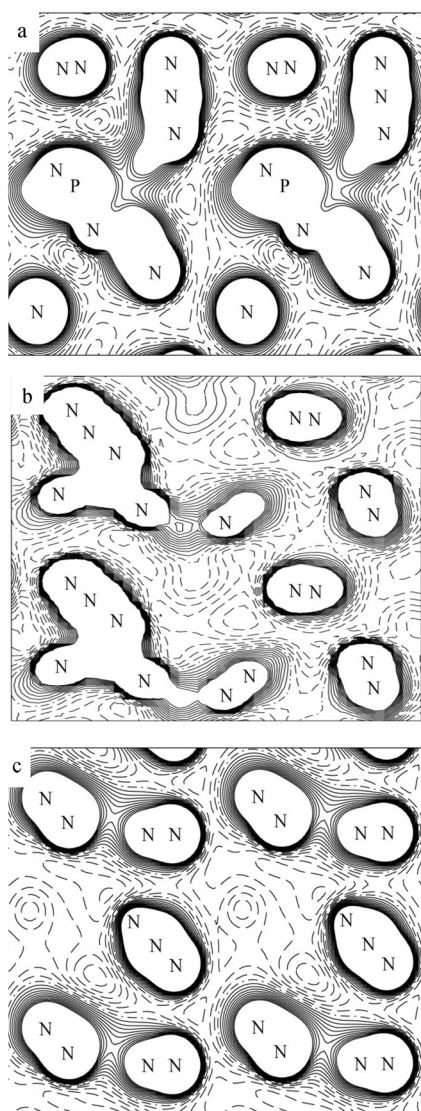


Figure 5 The point charge electrostatic potential of the bulk P_3N_{21} in the plane, (a) (100), (b) (010) and (c) (001) crystalline faces. Continuous, dashed, and dot-dashed lines, respectively, refer to positive, negative, and zero values. Contour intervals at $0.01 \text{ e} \cdot \text{Bohr}^{-3}$.

bution of electrostatic potential is quite uneven. The point charge electrostatic potential is very high between the azido groups of the neighboring molecules, indicating that the crystal lattice in this position may be easily

broken and becomes the explosion center when P_3N_{21} is impacted. The overlap population of $P-N_\alpha$ bonds is the weakest, therefore the $P-N_\alpha$ bonds first rupture by external stimuli.

References

- 1 Liebig, J.; Wohler, F. *Ann. Chem. Pharm.* **1834**, *11*, 139.
- 2 Audrieth, L. F.; Steinman, R.; Toy, A. D. F. *Chem. Rev.* **1943**, *32*, 109.
- 3 Grundmann, C.; Rätz, R. Z. *Naturforsch. B* **1955**, *10*, 116.
- 4 Chang, M. S.; Matusko, A. J. *J. Am. Chem. Soc.* **1960**, *82*, 5756.
- 5 Räuchle, F.; Gayoso, M. *Ann. Fis.* **1970**, *66*, 241.
- 6 Allcock, H. R. *Chem. Rev.* **1972**, *72*, 315.
- 7 Müller, J.; Schröder, H. F. *Anorg. Allg. Chem.* **1979**, *450*, 149.
- 8 Allen, C. W. *Chem. Rev.* **1991**, *91*, 119.
- 9 Göbel, M.; Karaghiosoff, K.; Klapötke, T. M. *Angew. Chem., Int. Ed.* **2006**, *45*, 6037.
- 10 Becke, A. D. *J. Chem. Phys.* **1993**, *98*, 5648.
- 11 Lee, C.; Yang, W.; Parr, R. G. *Phys. Rev. B* **1988**, *37*, 785.
- 12 Dovesi, R.; Causa, M.; Orlando, R.; Roetti, C. *J. Chem. Phys.* **1990**, *92*, 7402.
- 13 Monkhorst, H. J.; Pack, J. D. *Phys. Rev. B* **1976**, *13*, 5188.
- 14 Ju, X. H.; Xiao, H. M. *J. Theor. Comput. Chem.* **2004**, *4*, 599.
- 15 Dovesi, R.; Saunders, V. R.; Roetti, C.; Orlando, R.; Zicovich-Wilson, C. M.; Pascale, F.; Civalleri, B.; Doll, K.; Harrison, N. M.; Bush, I. J.; Llunell, M. *CRYSTAL06*, University of Torino, Torino, Italy, **2006**.
- 16 Hoffmann, R. *Solids and Surface: A Chemist's View of Bonding in the Extended Structure*, VCH Publishers, New York, **1988**.
- 17 Kortus, J.; Pederson, M. R.; Richardson, S. L. *Chem. Phys. Lett.* **2000**, *322*, 224.
- 18 Politzer, P.; Murray, J. S.; Seminario, J. M.; Lane, P.; Grice, M. E.; Concha, M. C. *J. Mol. Struct. (Theochem)* **2001**, *573*, 1.
- 19 Murray, J. S.; Lane, P.; Politzer, P. *Mol. Phys.* **1998**, *93*, 187.
- 20 Murray, J. S.; Lane, P.; Politzer, P. *Mol. Phys.* **1995**, *85*, 1.
- 21 Rice, B. M.; Hare, J. J. *J. Phys. Chem. A* **2002**, *106*, 1770.
- 22 Ji, G. F.; Xiao, H. M.; Dong, H. S. *Acta Chim. Sinica* **2002**, *60*, 194 (in Chinese).

(E0711212 SUN, H. P.)